

The Problem of Gulf Stream Separation: A Barotropic Approach

JOACHIM DENG

Institut für Meereskunde an der Universität Kiel, Kiel, Germany

(Manuscript received 1 April 1992, in final form 6 November 1992)

ABSTRACT

Inertial separation of a western boundary current from an idealized continent is studied in a homogeneous ocean circulation model. A number of processes are identified that either encourage or prevent separation at a coastal promontory in this model. For a single-gyre wind forcing a free-slip boundary condition forces the stream to follow the coastline, whereas the no-slip condition allows separation at a sharp corner. A prescribed countergyre to the north of the stream is not necessary to achieve separation if the no-slip condition is used. "Premature" separation occurs for wind fields that do not extend beyond the latitude of the cape. For a more realistic wind field and coastline two distinct states of the stream are found. At small Reynolds numbers the current fails to separate and develops a stationary anticyclonic meander north of the cape. Stronger currents separate and drive a recirculation in the lee of the continent.

1. Introduction

The Gulf Stream's separation from the North American coast at Cape Hatteras and its subsequent mean path are well established from observations (Maul et al. 1978; Auer 1987). The current leaves the continent on a straight path without any visible deflection at the separation point. However, eddy resolving ocean models that are quite capable of simulating meandering and ring formation after the current has left the shelf very often fail to reproduce this separation. Instead, they show a Gulf Stream that continues along the American coastline north of Cape Hatteras almost up to Georges Bank, where it forms a large stationary anticyclonic meander (Holland 1987; Thompson and Schmitz 1989; Bryan and Holland 1989). At the same time, however, there are also models that seem to produce a nicely separated Gulf Stream (Holland 1986; Mellor and Ezer 1991).

The failure of a boundary current to separate is not just a feature of Gulf Stream models. It has also been encountered in models of the Agulhas Retroflexion (De Ruijter and Boudra 1985; Boudra and Chassignet 1988). As the physics of boundary current separation are not well understood (Hendershott 1987), it is not known if the mechanism of separation should be the same in both cases. It is also not clear why some models seem to do better than others in reproducing the observed separation. However, with the growing number of large-scale high-resolution models (Bryan and Holland 1989; Böning et al. 1991; the FRAM Group

1991), the demands on the realism of the model output increase, stressing the need for a solution of the separation problem.

This paper is intended as a contribution to improve our understanding of boundary current separation in ocean circulation models and of the physics that may be playing a role in the separation of the real Gulf Stream. It was felt that the best way to achieve this aim is to take a step by step approach to the problem, where—starting from the most basic mechanisms—additional factors are gradually included into a numerical model. As a first step, a barotropic model will be used in this paper. An attempt will be made to isolate several of the different processes that interact at Cape Hatteras and to study their individual contribution to the stream's separation, in the model. It will be shown that even in this simple situation the nonlinear interaction of some model components produces effects that one should be aware of when trying to understand more complex models and the behavior of the real Gulf Stream.

2. The physical situation at Cape Hatteras

To introduce the processes that can be playing a role in the Gulf Stream's separation, a brief description of the physical situation in the vicinity of Cape Hatteras is necessary. This will also give an impression of the number of different aspects a realistic model would have to take into account.

From Miami to Cape Hatteras, the Gulf Stream (Florida Current) follows the American coastline rather closely. It stays on the shelf region of the Blake Plateau, with water depths of less than 1000 m. Vertically, the stream extends to the bottom (Leaman et al. 1989).

Corresponding author address: Joachim Dengg, Institut für Meereskunde an der Universität Kiel, Düsternbrooker Weg 20, 2300 Kiel 1, Germany.

At Cape Hatteras, the continent recedes to the north, but the stream continues along its course on a great circle (Fofonoff 1981), crosses the shelf break and the western boundary undercurrent (Richardson 1977), and begins to meander and shed warm and cold rings. Bottom depths here exceed 4000 m, but the stream's core with velocities greater than 10 cm s^{-1} stays above 1000 m (Halkin and Rossby 1985; Leaman et al. 1989). The Gulf Stream near Cape Hatteras is highly energetic with velocities of up to 1.6 m s^{-1} (Richardson 1977; Leaman et al. 1989). Even speeds of 1.8 m s^{-1} are reported in the literature (Richardson and Knauss 1971). The time mean of the total transport at Cape Hatteras is estimated to be 94 Sv ($\text{Sv} \equiv 10^6 \text{ m}^3 \text{ s}^{-1}$) (Leaman et al. 1989), with instantaneous values of up to 150 Sv farther downstream at 55°W (Richardson 1985). To the north of the Gulf Stream cold shelf water moves southwest with speeds of about $5\text{--}10 \text{ cm s}^{-1}$ (Beardsley and Boicourt 1981) and a northern recirculation gyre with a volume transport of about 20 Sv fills the Middle Atlantic Bight (Hogg et al. 1986).

The separation point at Cape Hatteras and the Gulf Stream's subsequent course coincide roughly with the annual mean position of the line of zero wind stress curl (Leetmaa and Bunker 1978; Fofonoff 1981). To the north of the Gulf Stream cyclonic vorticity is supplied to the ocean with a local maximum in the Middle Atlantic Bight (MacVeigh et al. 1987).

There is a large number of theories on the mechanisms of the Gulf Stream's separation [for a review see Haidvogel et al. (1992)], most of which tend to attribute the separation to one of the physical factors listed above, such as the curvature of the coastline, the shelf break, or the wind field. However, as yet there is no complete theory, and it is not clear if any one of the processes described in the literature determines the separation all by itself or if a combination of several of them is necessary to explain the observed path of the current.

The Gulf Stream's failure to separate in numerical models could result from a neglect or misrepresentation of some necessary physical process, but numerical reasons may also be playing a role. For example, the choice of model formulation (layer or level) has been shown to affect separation from the western boundary to some degree (Chassignet and Gent 1991), and low grid resolution has also been mentioned as a possible influence (Bryan and Holland 1989; Treguier 1992).

The results described in this paper suggest that the Gulf Stream's separation at Cape Hatteras is the product of a complex interaction of several physical factors, making the problem difficult to treat with analytical tools. It will be shown that separation is possible in the barotropic model for boundary currents that are sufficiently nonlinear to allow "inertial overshooting" at a coastal promontory. Future work will have to determine whether this type of separation can also take place in more realistic models and if the Gulf Stream's separation is indeed controlled by this mechanism.

3. The numerical model

Barotropic models are commonly used to gain some understanding of the role of specific processes in more complex models and the real ocean (e.g., Blandford 1971; Harrison and Stalos 1982; Marshall 1984; Böning 1986; Moro 1988). By leaving out thermohaline effects and baroclinic processes they are restricted to only a few physical components and thus have the advantage of being small in terms of computing space and time. In addition, their physics are believed to be quite well understood.

The barotropic model can be regarded as a representation of the vertically integrated, wind-driven part of the circulation above the main thermocline (Pedlosky 1979). It is based on the barotropic vorticity equation in a homogeneous flat-bottom ocean:

$$\frac{\partial \zeta}{\partial t} + \mathbf{u} \cdot \nabla \zeta + \beta_0 v = \mathbf{k} \cdot \frac{\nabla \times \boldsymbol{\tau}}{\rho_0 H_0} - r \zeta + A_H \nabla^2 \zeta, \quad (1)$$

NONL BETA WIND FRIC DIFF

where NONL denotes the nonlinear advection of relative vorticity, BETA the planetary vorticity term, WIND the wind stress vorticity, FRIC the vorticity losses by bottom friction, and DIFF the horizontal diffusion of vorticity. The symbols used are explained in Table 1.

The geostrophic velocity \mathbf{u} is related to the geostrophic pressure p by

$$u = -\frac{1}{\rho_0 f_0} \frac{\partial p}{\partial y}, \quad v = \frac{1}{\rho_0 f_0} \frac{\partial p}{\partial x}. \quad (2)$$

Note that p is equivalent to a streamfunction ψ by

$$\psi = \frac{p}{\rho_0 f_0}. \quad (3)$$

In this paper p shall be used as a streamfunction.

The vorticity equation (1) is solved subject to the boundary conditions of no flux

$$p = 0, \quad (4)$$

TABLE 1. Symbol definitions.

$\mathbf{u} = (u, v)$	vertically integrated horizontal velocity
$\zeta = \frac{\partial v}{\partial x} - \frac{\partial u}{\partial y}$	relative vorticity
\mathbf{k}	unit vertical vector
$\boldsymbol{\tau}$	wind stress vector
ρ_0	reference density: $\rho_0 = \text{const}$
H_0	constant depth
r	coefficient of bottom friction
A_H	coefficient of turbulent horizontal diffusion
$\nabla = \left(\frac{\partial}{\partial x}, \frac{\partial}{\partial y} \right)$	horizontal gradient operator
$f_0 + \beta_0 y$	planetary vorticity
p	geostrophic pressure

and either no slip

$$\mathbf{u} = 0, \quad (5)$$

or free slip

$$\frac{\partial \mathbf{u}}{\partial \mathbf{n}} = \zeta = 0, \quad (6)$$

(where \mathbf{n} is the local coordinate normal to the boundary).

The domain considered is a closed rectangular basin with a simplified continent in the west. The horizontal resolution of $1/4 \text{ deg} \times 1/4 \text{ deg}$ (corresponding to $23 \text{ km} \times 28 \text{ km}$ in x and y for a reference latitude of 35°N) was chosen such that the western boundary current with a typical width of about 120 to 170 km at Cape Hatteras (Leaman et al. 1989) is well resolved, while at the same time a closed box can be used to avoid influences of open boundaries. The constant depth is 1000 m, which, as pointed out in section 2, corresponds to the Gulf Stream's high velocity core. The basin extends from 15° to 55°N , 25° to 80°W to simulate realistic dimensions of the North Atlantic. The time step used for integration is 32 min.

Coefficients of bottom friction and horizontal turbulent diffusion vary in different experiments and will be given later. Generally, their relative magnitudes are chosen such that the western boundary layer is diffusive, that is, dominated by the balance of BETA and DIFF in (1). Consequently, the resulting characteristic scale is the diffusive length scale given by

$$\delta_L = \left(\frac{A_H}{\beta_0} \right)^{1/3}, \quad (7)$$

as shown by Pedlosky (1979).

Near the separation point, the Reynolds number

$$\text{Re} = \frac{UL}{A_H} \quad (8)$$

will be of interest. It gives the magnitude of the advection terms relative to the diffusion term in the vorticity equation (1). To determine Re , U and L are taken from the model results.

Values of A_H are determined by requiring the no-slip current at the western boundary to decelerate from its maximum speed to zero in more than just the last grid interval.

Unless stated differently the wind stress curl is a simple sine function in y and constant in x , producing a single anticyclonic gyre (Fig. 1). The amplitude of the wind stress curl varies from 0.5 to $20.0 (\times 10^{-7} \text{ Pa m}^{-1})$ in different experiments.

The numerical method is standard leapfrog integration in time (Roache 1976). Central differences are used for horizontal derivatives and the Arakawa scheme conserving energy and enstrophy is applied to the advective terms (Bengtsson and Temperton 1979). The Poisson equation relating p and ζ is solved with an SOR method. Numerical treatment of the no-slip condition is the first-order method documented in Roache (1976), while his method no. 3 is used at sharp convex corners. As shown by Foreman and Bennett (1988), first-order schemes for the no-slip condition are as accurate as a local third-order estimate.

The model was integrated to a statistically steady state, as diagnosed from the integral kinetic energy. Mean fields were calculated over sufficiently long periods to average out basin modes, eddies, and other transients. Only the time mean fields over at least one year will be considered, because the Gulf Stream's sep-

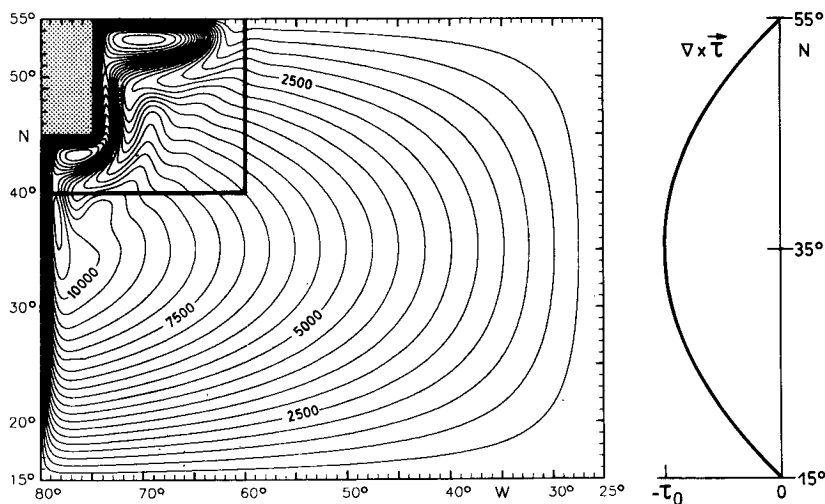


FIG. 1. Streamfunction (in Pa) (cf. section 3) for $\text{Re} = 60$ (contour interval 500 Pa). The box from 40° to 55°N , 60° to 80°W indicates the area of the model region shown in the next figures. The wind stress curl is a function of latitude only ($\tau_0 = 5 \times 10^{-7} \text{ Pa m}^{-1}$).

aration is a steady phenomenon (Auer 1987) that should be identifiable as a mean state of the model.

Although well suited for process studies, the barotropic model will allow only limited conclusions with respect to the separation of the real Gulf Stream. To accelerate a homogeneous water column of 1000-m depth to realistic speeds (1 m s^{-1}), an unrealistically large wind forcing has to be applied, resulting in too large mass transports. The model current obtained in this way is not readily comparable to observations. In addition, variable bottom topography cannot be included because a barotropic stream is closely tied to f/H contours, whereas a baroclinic current is not (Holand 1973).

4. Separation at sharp corners

To simplify the discussion, throughout this paper the term "separation" is defined as the complete detachment of a boundary current from the coast. With this definition, none of the streamlines is allowed to remain in contact with the boundary downstream of the separation point.

In the past, the separation of model boundary currents has usually been associated with a straight meridional western boundary (Moro 1988; Cessi 1990; Cessi et al. 1990; Chassignet and Gent 1991; Rhines and Schopp 1991; Haidvogel et al. 1992). Consequently, it was either a forced separation due to convergence of two boundary currents or it resembled the classical results on the separation from flat plates (Batchelor 1967).

However, the Gulf Stream does not separate from a straight coast. The introduction of a coastal promontory like Cape Hatteras allows "inertial separation," that is, an overshooting of the fluid parcels at the sharp corner due to their large momentum. In this paper I will try to demonstrate some effects associated with this type of separation.

a. Effects of nonlinearity and boundary conditions

The concept of nonlinear currents separating at sharp corners is not new: Batchelor (1967) already presented a number of tank experiments that show how an increase of the Reynolds number Re of the flow leads to separation and the development of a "standing eddy" in the lee of an obstacle. After separation the current begins to meander and forms a turbulent wake. Batchelor states that this behavior is found for Re greater than order 10, depending on the shape of the object.

The Gulf Stream's flow pattern at Cape Hatteras is very similar to these tank experiments. Furthermore, the Stream is generally regarded as an inertial jet (Warren 1963; Robinson and Niiler 1967; Luyten and Robinson 1974; Fofonoff 1981), carrying its own energy and momentum into the region northeast of Cape Hatteras. So it does not seem unreasonable to expect

that the Gulf Stream's separation might be inertially controlled and that a numerical model at sufficiently large Reynolds number should be able to produce a separated jet and the associated recirculation region in the lee of the continent.

Bryan (1963) tested this hypothesis by putting a rectangular continent into his model and applying an anticyclonic wind field over the whole basin. At $Re = 60$ he found the type of behavior shown in Fig. 1: the zonal boundary current does not separate at the cape but makes a 90° turn to the north, without losing contact with the coast. Only a small part of the stream recirculates south of the corner, intensifying the boundary current there. This result lead Bryan to conclude that the coastline has only a minor effect on separation. He assumed that the Reynolds number in his experiments was too small to produce a cyclonic recirculation cell in the wake of the continent.

The validity of this conclusion was examined by using Bryan's rectangular continent in a series of experiments shown in Fig. 2. In all model runs the same values for the coefficients of diffusion ($A_H = 1500 \text{ m}^2 \text{ s}^{-1}$) and bottom friction ($r = 2.5 \times 10^{-7} \text{ s}^{-1}$) have been used. The magnitudes were chosen according to the requirements described in section 3. The main results of this section, however, do not depend on the particular choice of parameters, as shall be shown below. The amplitude of the wind stress curl is given in the figures as a fraction of $\tau_0 = 5.0 \times 10^{-7} \text{ Pa m}^{-1}$. (Note that the contour interval of the streamfunction is not the same in all figures.)

At small Reynolds numbers the streamline pattern in the lee of the continent is more or less that of linear experiments (Figs. 2a,b): streamlines leave the western coast not as a concentrated current but individually when the flow has lost its relative vorticity at the boundary. Only a slight overshooting can be observed. At $Re = 15$ a small recirculation cell forms south of the continent, and with increasing Re it intensifies (Fig. 2c) and is drawn around the cape. For large Reynolds numbers ($Re = 60$) Bryan's circulation is reproduced (Fig. 2d) with a northern boundary current and a second recirculation cell there. If the wind forcing is increased still further (to values that are very large but justifiable in the context of a process study), the northern boundary current strengthens (Fig. 2e) and finally reaches the eastern boundary as in the experiments of Veronis (1966). However, a well-defined separation of the stream cannot be detected at any Reynolds number. Contrary to the results of the tank experiments the current in the numerical model can obviously become very nonlinear without separating from the coast. What causes this unexpected behavior?

Bryan (1963) used "free slip at the upper (poleward) and lower (equatorward) boundaries, and no slip at the lateral (eastern and western) boundaries." As the southern coast of the continent is a poleward boundary, it is very likely that free slip was used there too (Bryan, personal communication), although this is not explic-

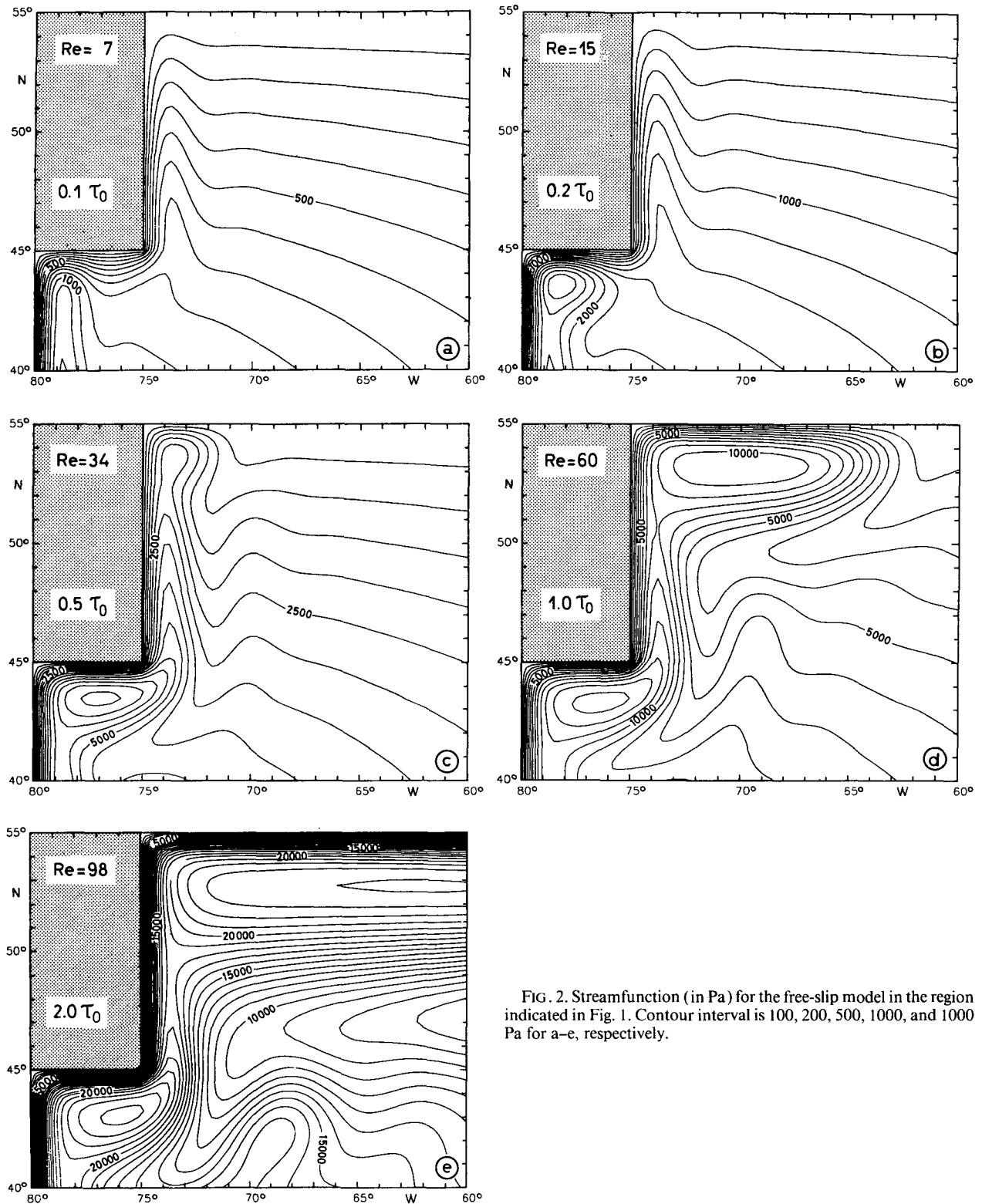


FIG. 2. Streamfunction (in Pa) for the free-slip model in the region indicated in Fig. 1. Contour interval is 100, 200, 500, 1000, and 1000 Pa for a–e, respectively.

itly stated in the paper. For the model runs of Fig. 2 the free-slip condition was used at all horizontal boundaries.

If the same set of experiments is repeated with a no-slip boundary condition at the western border and along the continent, we find a completely different cir-

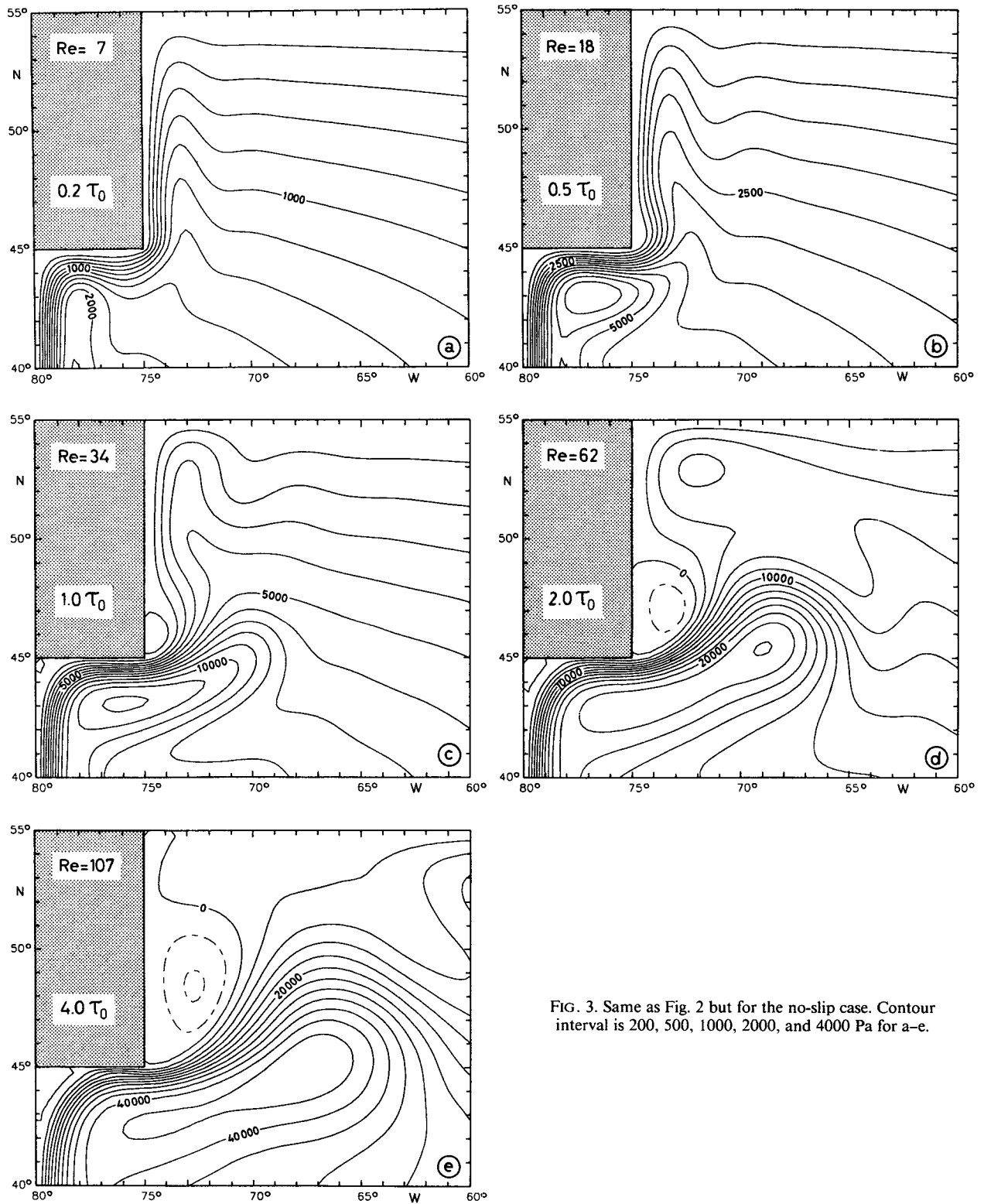


FIG. 3. Same as Fig. 2 but for the no-slip case. Contour interval is 200, 500, 1000, 2000, and 4000 Pa for a–e.

culatation pattern (Figs. 3a–e): for Reynolds numbers greater than about 10 the stream now separates at the cape, continues for some time on its zonal course, and

forms a “northern recirculation cell” in the lee of the continent. At $Re = 18$ (Fig. 3b) the separation is not very pronounced yet, but with increasing Re (Fig. 3c–

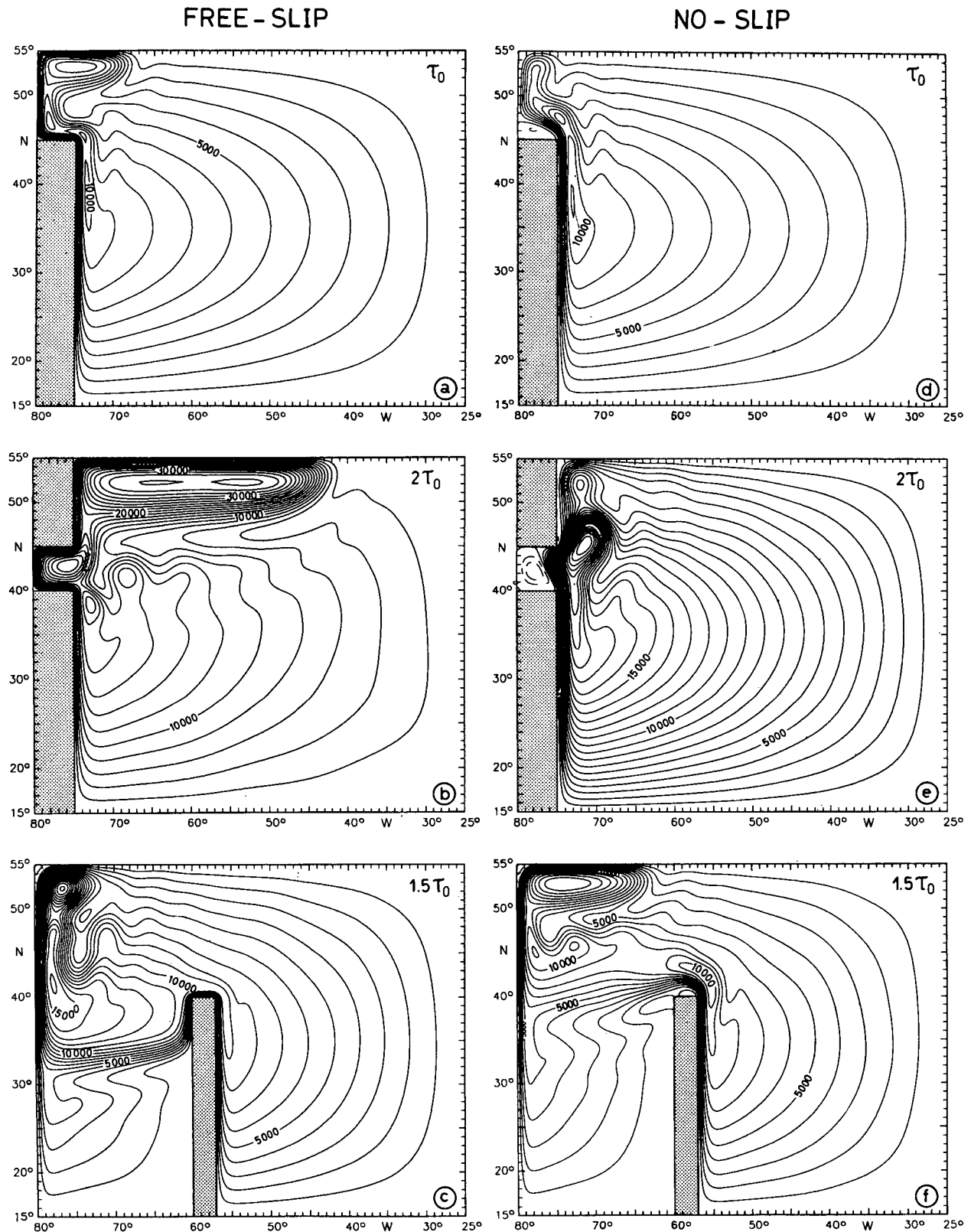


FIG. 4. Free-slip runs (left) and no-slip (right) with different continents, wind forcing, and different values of the parameters A_H [$\text{m}^2 \text{s}^{-1}$], r [s^{-1}] (a, d) 1500, 2.5×10^{-7} ; (b, e) 5000, 10.0×10^{-7} ; (c, f) 800, 1.0×10^{-7} . Contour interval is 1000 Pa except for Fig. 4b where it is 2000 Pa. Wind forcing is given in multiples of $\tau_0 = 5 \times 10^{-7} \text{ Pa m}^{-1}$.

e) it becomes obvious. Note that the separation point does not change its position at different Reynolds numbers. For small Re (Fig. 3a) there is no clear separation and the picture is similar to the free-slip case. These patterns produced by the no-slip condition agree much better with the results of the tank experiments (Batchelor 1967) than the free-slip model runs.

This result is not coincidental. Different geometries and different values of the parameters were used to demonstrate the failure of the free-slip condition to allow inertial separation (Fig. 4a–c). In none of these situations does the current leave the coast. The same runs with no slip along the continents produce separation in all cases (Fig. 4d–f). The same phenomenon has also been encountered in the attempts to model the Agulhas Retroflection (De Ruijter and Boudra 1985), in the Werner et al. (1988) model of the Alboran Gyre and in Cummins and Mysak's (1988) model of the Alaskan Gyre. [Figures 4c and 4f are basically Northern Hemisphere versions of De Ruijter and Boudra's (1985) South African continent.] Clearly, the difference between the two boundary conditions is a fundamental one and not caused by a special combination of the free parameters.

Analytical calculations confirm this peculiarity of the free-slip boundary condition. Cherniawsky and LeBlond (1986) examine the behavior of nonlinear free-slip currents at sharp corners and find a stream that turns around the corner without any noticeable separation.

Lower horizontal resolution did not severely affect the results of these numerical experiments. Different runs were performed, but even in the case of a poorly resolved boundary layer (1° model; not shown here) separation was obtained in the no-slip case, whereas the free-slip current stayed at the coast independent of the grid spacing used.

To understand this difference in the separation behavior of free- and no-slip boundary currents, consider streamlines $S1$ and $S2$ in Fig. 5. Streamline 1 is assumed to be the bounding streamline of the northern recirculation cell, and $S2$ that of the subtropical gyre and therefore of the separated boundary current. (For simplicity's sake it shall be assumed that $S1$ lies in the boundary layer in the north and west and is in contact with $S2$ in the south and east as indicated in Fig. 5.)

The vorticity necessary to maintain the recirculation cell $S1$ must be provided by the separated boundary current. This can be shown by integrating the barotropic vorticity equation (1) over an area bounded by a closed streamline, giving

$$\frac{1}{\rho_0 H_0} \oint_{\psi} \tau \cdot d\mathbf{l} - r \oint_{\psi} \mathbf{u} \cdot d\mathbf{l} + A_H \oint_{\psi} (\nabla \zeta \cdot \mathbf{n}) dl = 0 \quad (9)$$

for the steady state, as shown, for example, by Pedlosky (1979). (Here $d\mathbf{l}$ is an infinitesimal vector line element tangent to $\psi = \text{const}$, and \mathbf{n} is the unit vector normal

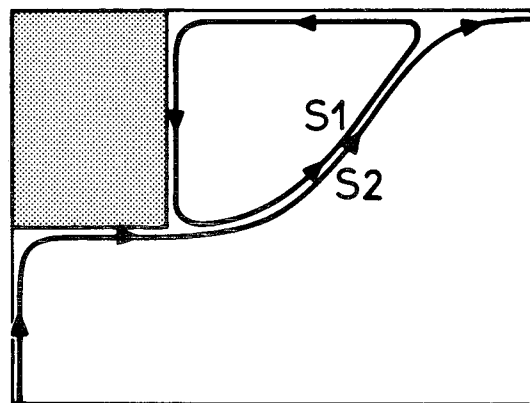


FIG. 5. Schematic sketch of a separated inertial jet; $S1$ denotes a streamline in the recirculation cell; $S2$ is a streamline of the western boundary current.

to the streamline.) The planetary vorticity and the advection terms do not contribute to the balance when integrated around a closed gyre.

Consider the individual terms of balance (9) for the cell $S1$: integrating around it in a cyclonic sense, the contribution of the wind field is negative, as $\text{curl} \tau$ is assumed to be anticyclonic over the whole basin. The bottom friction term is also negative because $\mathbf{u} \cdot d\mathbf{l}$ is always positive along the streamline. This means that the net diffusion must be positive.

However, inside the boundary layers in the north and west negative vorticity generated by the boundary is spread into the cell by the diffusion term (Batchelor 1967). (This is true for both the free and the no-slip condition.) So the only place where diffusion can supply the necessary positive vorticity to the standing eddy is along $S2$. Consequently, the separated boundary current must be able to pass on cyclonic vorticity to the cell.

For the no-slip current this is no problem because it leaves the coast with the profile sketched in Fig. 6a: on the current's coastal flank it has positive relative vorticity, which was created by the no-slip boundary and is advected with the stream by the nonlinear term. This vorticity can subsequently be diffused into the recirculation cell. (Details will be given below.)

The free-slip current has the profile shown in Fig. 6b: the relative vorticity at a free-slip coast is identically zero due to condition (6) and negative everywhere in the boundary current. If this stream could separate as indicated in the diagram, advection would carry its negative vorticity into the region of contact of $S1$ and $S2$. In this case there would not be any positive vorticity for the free-slip stream to deliver to the cell. In fact, if it came into contact with a cyclonic recirculation cell, positive vorticity from the cell would be diffused into the separated current rather than out of it. In a time-dependent situation this would drain the vorticity from the cell until the eddy disappears. (This has been confirmed by numerical experiments not shown here.) In

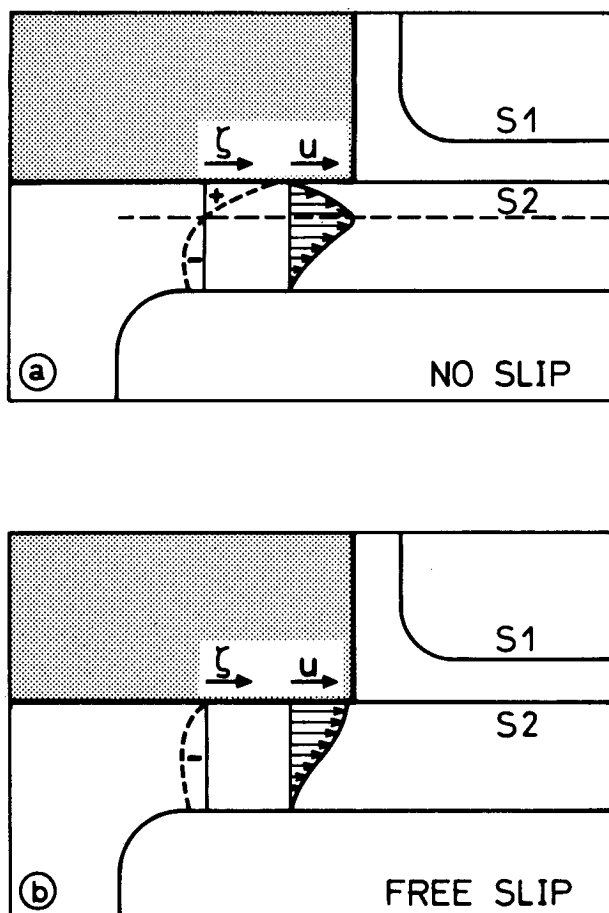


FIG. 6. Sketch of the separation situation with different boundary conditions, showing cross-stream profiles of the relative vorticity ζ and the zonal velocity u . (a) No-slip situation. Broken line denotes axis of stream. (b) Hypothetical free-slip situation.

the steady state considered above, the cell simply cannot exist because it does not have a source of vorticity.

However, if the free-slip stream is not able to supply positive vorticity to the region in the lee of the separation point, it cannot separate in the sense defined above and form a free inertial jet. Its only alternative at the cape is then to turn around the corner in the way found in the experiments (Fig. 2).

If there is an external source of positive vorticity to the north of the cape, separation should become possible also for the free-slip stream, depending on the strength of the forcing. In models this is often achieved by use of a double-gyre wind field, which will be examined more closely in section 4d. However, with a no-slip condition, single-gyre forcing is sufficient to produce separation at a sharp corner. An externally driven counter-gyre north of the Gulf Stream is not a necessary condition for separation to occur in this model.

Note that the argument presented above holds for flow in any geographical direction, because the effect

of the planetary vorticity does not appear in the integration along closed streamlines. In addition, it is independent of the relative magnitudes of the terms in the vorticity equation: the difference in the effect of free and no slip is caused by the boundary conditions alone and not by a particular choice of regime (diffusive, frictional, inertial). The dominant dynamical balance in the barotropic flat-bottom separation problem is that between diffusion and advection of relative vorticity. This is illustrated in Fig. 7 showing the magnitude of the individual terms of the vorticity equation along sections A (before separation) and B (after) for the case of Fig. 3c. Vorticity is created at the no-slip boundary, diffused into the whole boundary current ($\text{DIFF} > 0$) and advected to the point of separation ($\text{NONL} < 0$). After separation, the signs of the diffusive and advective terms in the vorticity equation reverse (Fig. 7, section B): vorticity that is supplied by advection is diffused out of the free jet into the surroundings. Note that the diffusion on the left flank of the current is much more intensive than on the right and that the high positive vorticity along the coast is very quickly reduced after separation. This role of the nonlinear terms as the transport mechanism for vorticity generated at the boundary explains why there is no pronounced separation at small Reynolds numbers (Fig. 3).

The steady state considered in this paper is of course an idealized situation. In reality, large Reynolds numbers also mean a high degree of temporal variability of the separated current. However, the separation itself as well as the cyclonic recirculation cell are always present in instantaneous pictures (not shown here).

To summarize the effects of the lateral boundary conditions and the nonlinearity, one can state that the introduction of a sudden change of the orientation of the coastline is not sufficient to produce inertial separation in a barotropic model. To leave the coast at a sharp corner, the stream has to be able to supply vorticity to the circulation in the lee of the continent. This is impossible for a free-slip current. In the model considered here, separation by overshooting can only be achieved by the use of a no-slip condition in connection with a sufficiently high Reynolds number of the flow. However, given these factors, the presence of the cape enables a separation that is different from that in straight-coast models in two important respects: it takes place at a fixed location (the cape), and there is no need for an externally driven counter-gyre.

b. Role of bottom friction

In section 4a it was demonstrated that the systematic difference between the two dynamic boundary conditions is independent of the particular choice of model parameters. The details of the separation pattern achieved with the no-slip condition do, however, depend on parameters such as the coefficient of bottom friction.

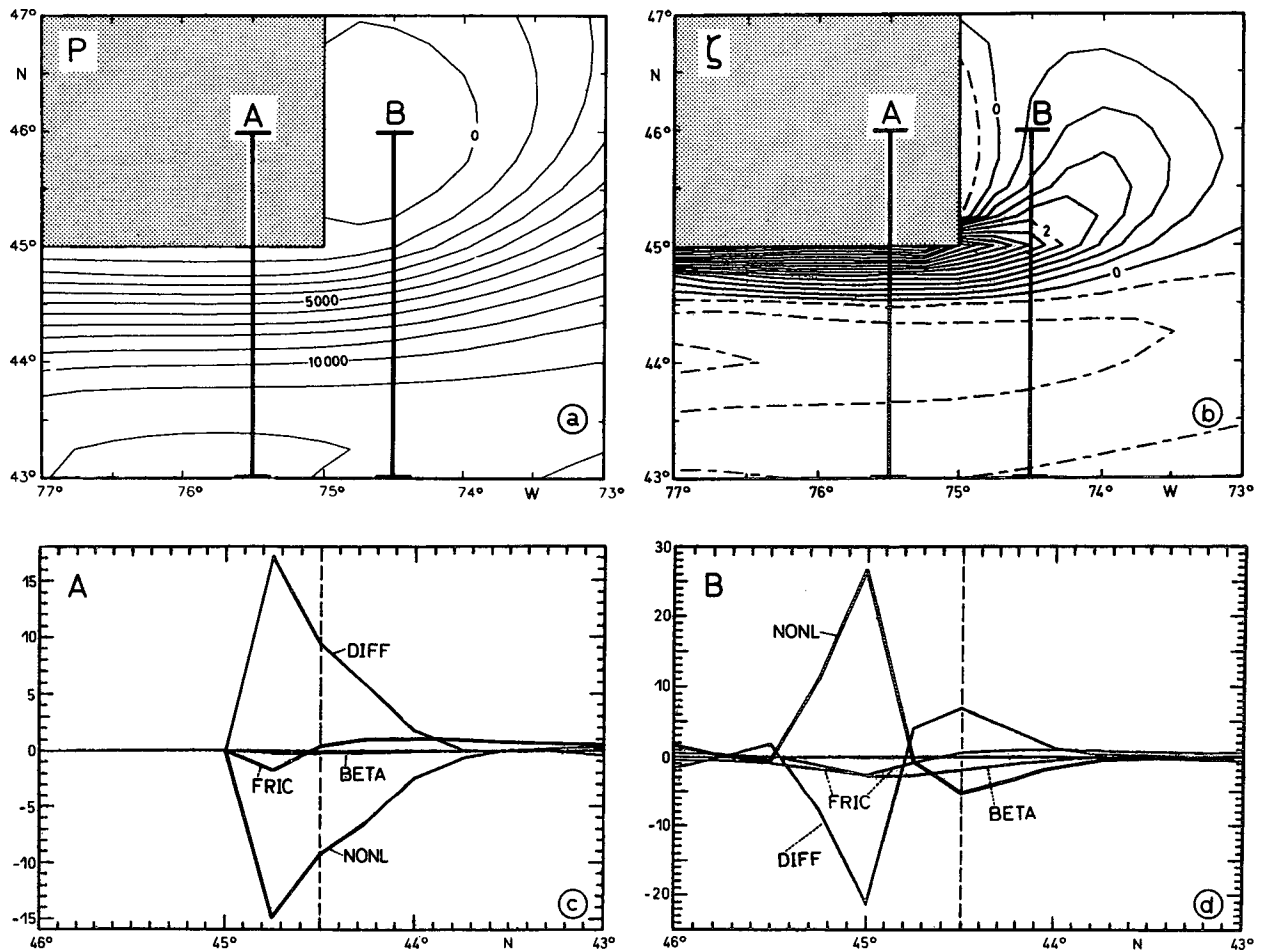


FIG. 7. Vorticity sections before and after separation for the situation shown in Fig. 3c. (a) Streamfunction in Pa near the separation point. Contour interval 1000 Pa. Lines A and B mark location of sections. (b) Relative vorticity ζ in s^{-1} . Contour interval $0.4 \times 10^{-5} s^{-1}$. Broken line indicates negative values. (c) Section A of individual terms in the vorticity equation (1) (multiplied by the time step to give units of vorticity): vertical line denotes stream axis ($\zeta = 0$). Abbreviations are defined in (1). Units: $10^{-8} s^{-1}$. (d) Same as in section A for section B.

As an example, Fig. 8a shows the standard run of Fig. 3c ($r = 2.5 \times 10^{-7} s^{-1}$) together with an experiment where the coefficient of bottom friction is 60% smaller (Fig. 8b, $r = 1.0 \times 10^{-7} s^{-1}$). With reduced bottom friction the zonal penetration of the free jet becomes larger and both the southern and northern recirculation cells are considerably stronger. Speeds in the boundary current increase by 25%; the relative vorticity and the magnitude of the diffusion term by approximately the same amount. This has to be compared with Fig. 3e, where stronger forcing produced current speeds that were 220% larger than in the reference case of Fig. 8a but did not show the same effect on separation as the smaller friction.

The growth of both recirculation cells with lower values of bottom friction can again be explained in terms of vorticity. The scale of the model boundary current is determined by diffusion because the influence of bottom friction was chosen to be small. Therefore a further reduction of r is not able to drastically change

the structure of the boundary current. However, almost everywhere in the recirculation cell bottom friction is an important sink for vorticity (apart from a thin diffusive layer at the boundary). So the change in r has considerable consequences in the interior of the cell: While the diffusive input of vorticity into the recirculation cell remains approximately the same, the smaller bottom friction is now less effective in destroying it. To make up for that it requires a correspondingly larger area over which to act.

Nevertheless, although the choice of bottom friction changes the details of the separation, for the diffusive regime considered here a change in bottom friction does not change the separation itself.

c. "Premature" separation

Attention will now be focused on a phenomenon that Blandford (1971) and Holland and Lin (1975) already addressed. In both of their models, a no-slip

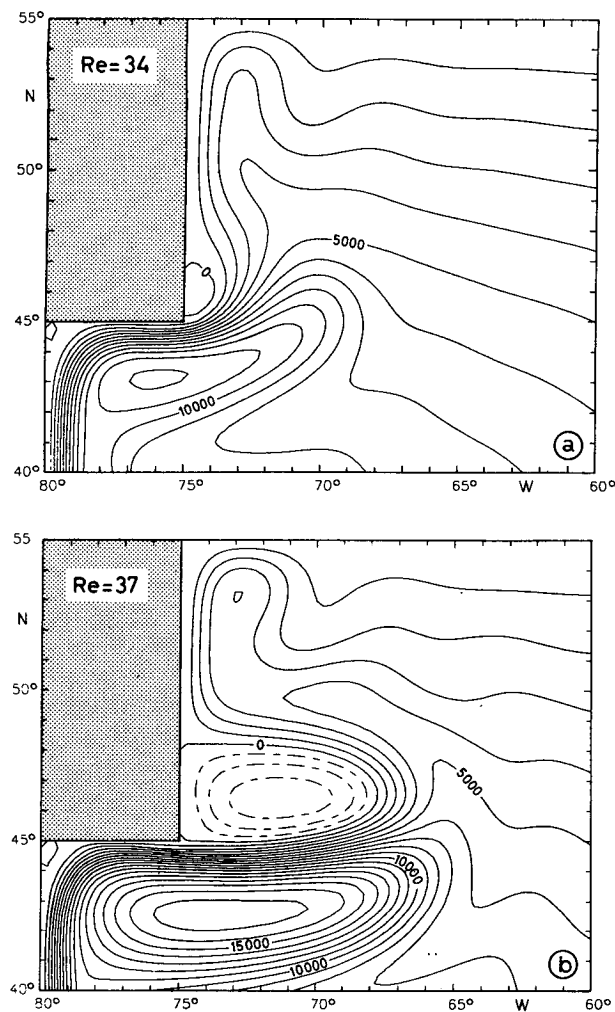


FIG. 8. (a) Streamfunction for standard no-slip run from Fig. 3c ($r = 2.5 \times 10^{-7} \text{ s}^{-1}$). (b) Streamfunction for lower value of bottom friction ($r = 1.0 \times 10^{-7} \text{ s}^{-1}$). Contour interval is 1000 Pa.

boundary current is not able to follow a zonal northern coast for a long distance, the way a free-slip current does (Veronis 1966). Instead, it separates forming a large anticyclonic recirculation cell south of the continent and a pattern of standing Rossby waves farther downstream. Holland and Lin (1975) concluded that this separation from the northern boundary is necessary to dissipate the stream's excess vorticity before it can return into the Sverdrup regime. Recently Marshall and Marshall (1992) demonstrated that this recirculation is a result of the current profile caused by the no-slip condition.

To show the consequences of this effect on inertial separation from a rectangular continent, the width of the continent was changed in the following set of experiments (Fig. 9). At a slim continent (Fig. 9a) the current separates in the way already shown in section 4a. If the zonal extension of the continent is increased, the stream forms an anticyclonic recirculation cell that

leaves the coast before the current can reach the cape (Fig. 9b). A further increase in the width of the continent (Fig. 9c) does not result in a significant change

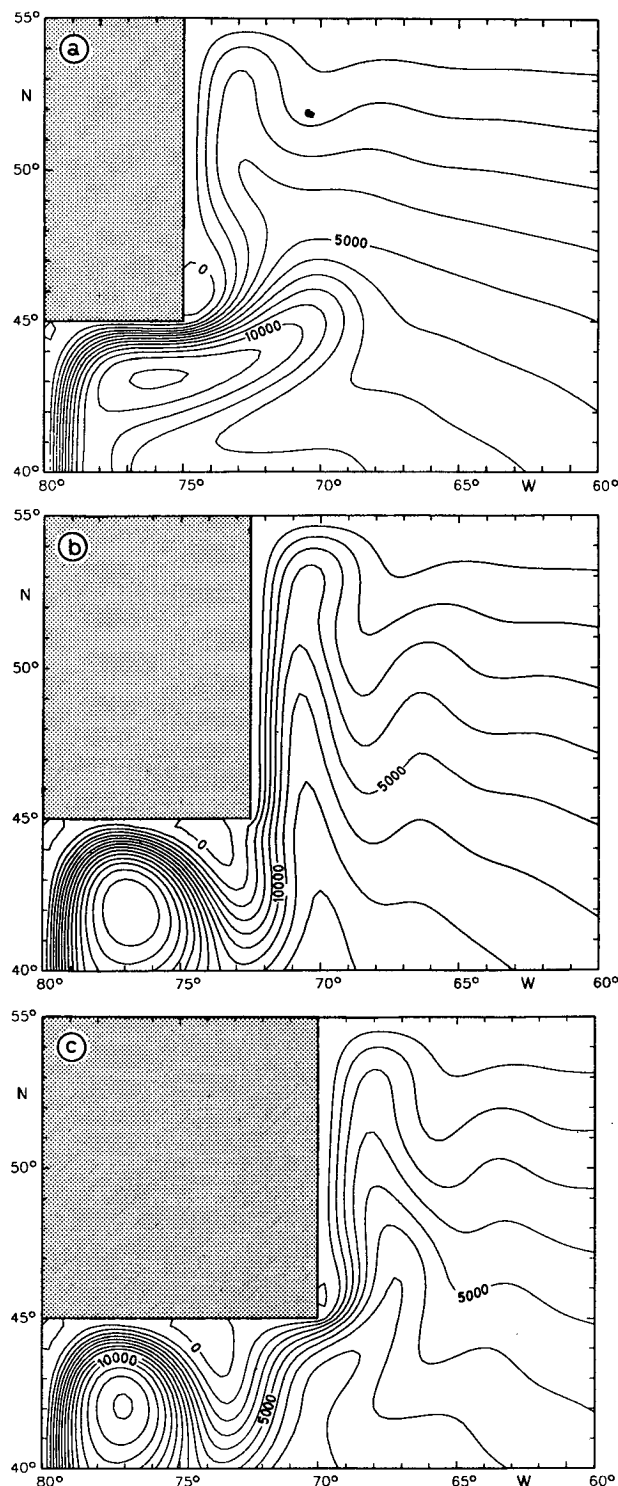


FIG. 9. Streamlines for standard parameter setting of Fig. 3c with different zonal extensions $\Delta\lambda$ of the continent: (a) $\Delta\lambda = 5.0^\circ$, (b) $\Delta\lambda = 7.5^\circ$, and (c) $\Delta\lambda = 10.0^\circ$. Contour interval: 1000 Pa.

of the cell's size. Farther downstream the current is still concentrated enough to separate at the cape if the crest of the next meander touches the continent near the corner (Fig. 9c). To distinguish this type of separation from the separation by "overshooting" at the cape, for the purpose of this paper it will be called "premature" separation (an expression borrowed from Haidvogel et al. 1992).

If the broad continent of Fig. 9b is used for different values of the wind forcing (Fig. 10a–c), the separation point moves downstream along the coast with increasing strength of the boundary current. The course of the separated current becomes more zonal, disguising the early separation to some degree, and the size of the anticyclonic recirculation cell south of the continent increases. Both the cell's radius and the distance of the separation point from the western boundary are determined by the inertial length scale

$$\delta_I = \left(\frac{U}{\beta_0} \right)^{1/2}, \quad (10)$$

as shown in the figures.

The interpretation of these results is that a long zonal no-slip coast effectively acts like a no-slip northern boundary, and the stream tries to leave it in the characteristic anticyclonic cell ("modon" solution, Marshall and Marshall 1992). If the zonal extension of the continent is smaller than the diameter of the inertial recirculation cell (Figs. 9a, 10c), the current can leave the no-slip coast at the cape without having to change its direction.

Of course, the American coastline near Cape Hatteras is not zonal and is therefore better approximated by a wedge-shaped continent (Fig. 11) similar to that used by Cox (1985). To allow comparisons with the last set of experiments, the line of vanishing wind stress curl again lies at the northern boundary, whereas in Cox's case it was made to coincide with the latitude of the cape. At a first glance the same kind of separation behavior is obtained in Fig. 11 as at the rectangular continent (Fig. 10). The stream does not separate at the cape but is deflected from the coast in an anticyclonic recirculation cell. With increasing strength of the boundary current the cell grows in size and its radius is again determined by the inertial length scale. The maxima of current speeds in the boundary current are almost identical to those in Fig. 10. There is a marked difference, however, in that this time the separation point moves *upstream* with larger Reynolds numbers. Even for strong flows (Fig. 11c) the current is not able to reach the cape; in fact, it separates almost immediately at the oblique coast.

One is led to suspect that the cape's proximity to the northern boundary might influence the separation behavior in these experiments. This was examined by moving the leading edge of the continent 5° farther to the south. Whereas in the case of the rectangular continent "premature" separation occurred irrespective of

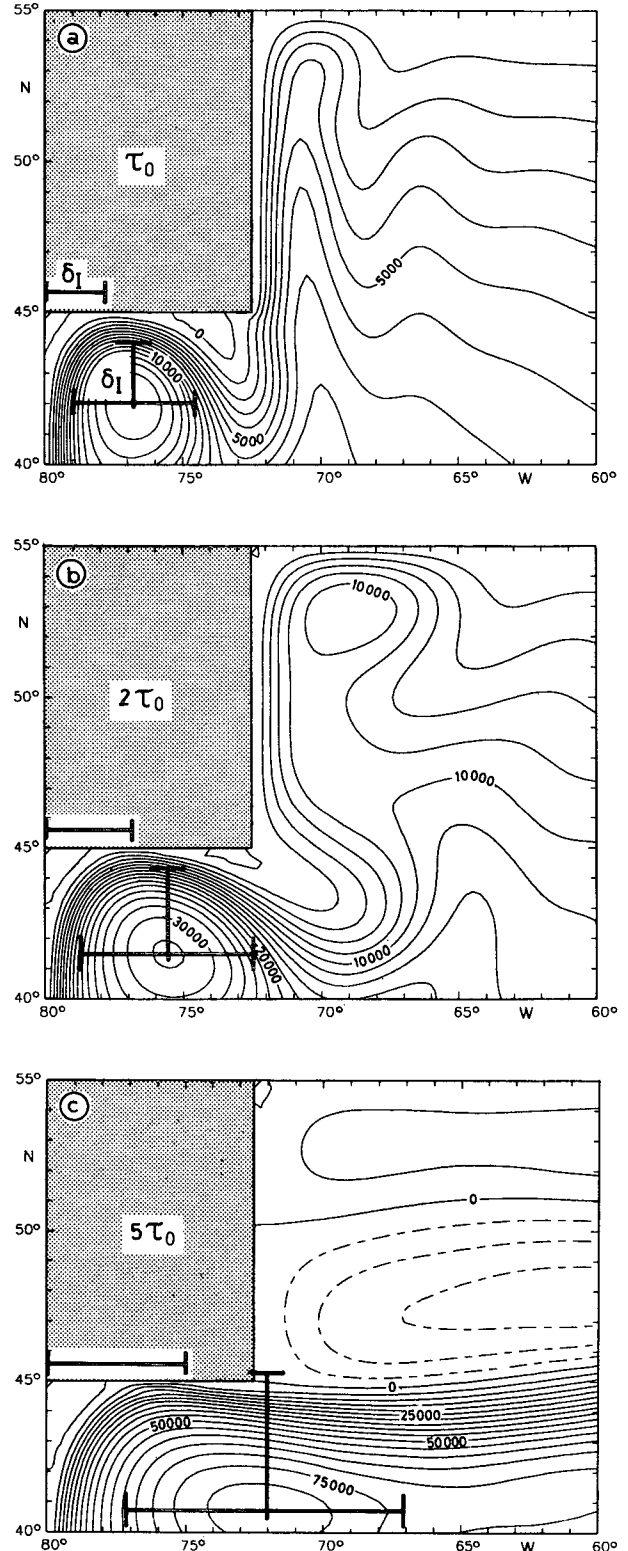


FIG. 10. Streamlines for a broad rectangular no-slip continent ($\Delta\lambda = 7.5^\circ$) at different values of wind forcing ($\tau_0 = 5 \times 10^{-7} \text{ Pa m}^{-1}$). Contour intervals are 1000 Pa, 2000 Pa, and 5000 Pa. The scales indicated in the plots give inertial length scale δ_I as defined in (10). Magnitudes of δ_I are 220, 316, and 500 km. Parameters are those from Fig. 3.

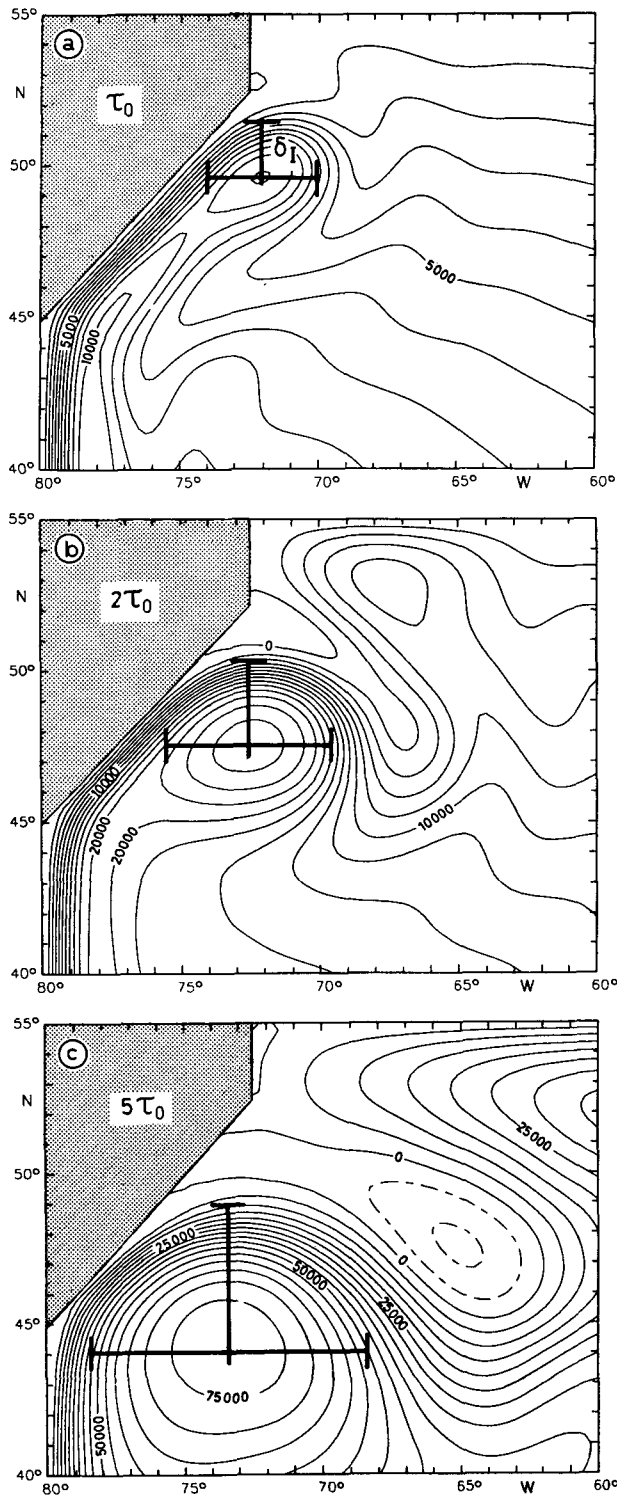


FIG. 11. Same as Fig. 10 but for wedge-shaped continent.

the continent's position relative to the northern boundary, for the wedge-shaped landmass position does play a role (Fig. 12): for all three values of wind forcing (Figs. 12a–c) the current now separates at the

cape. At high Reynolds numbers (Fig. 12c) the stream is even able to reach the northern (free slip) boundary as a concentrated jet.

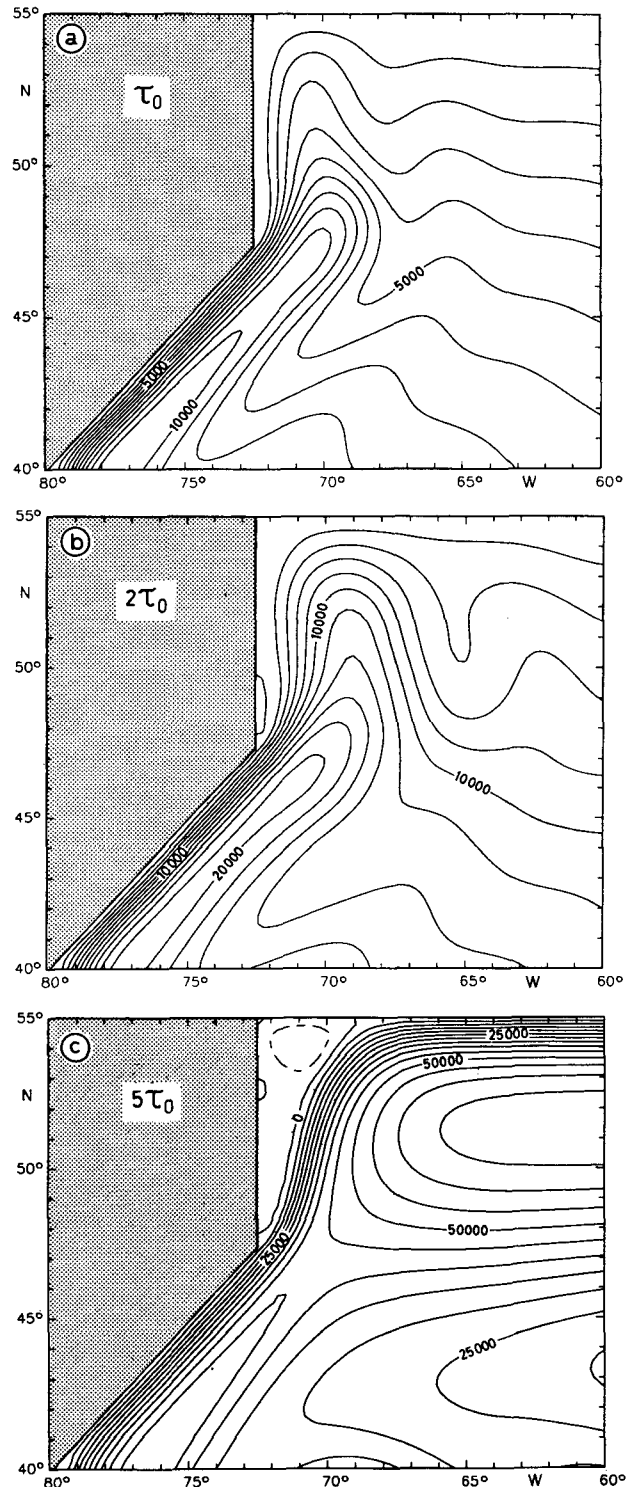


FIG. 12. Same parameters as in Fig. 11 but for a continent 5° farther south.

However, there are two factors that may be responsible for the dependence of the separation pattern on the latitude of the idealized continent. As already mentioned, one is the proximity of the northern boundary, which might have some kind of blocking effect; the other is the position of the cape in relation to the wind field.

To be able to examine the role of the wind field and to minimize the influence of the northern boundary, the sharp corner was positioned a long distance away from it at 37.5°N (Fig. 13). In Fig. 13a, $\text{curl}\tau = 0$ was chosen to coincide with the cape just as in Cox's (1985) experiments. Figure 13b has the line of zero wind stress curl 3° north of the coastal promontory, which makes it comparable to Fig. 11b, and in Fig. 13c, $\text{curl}\tau = 0$ is moved another 5° farther to the north to correspond to the situation in Fig. 12b. North of the line of zero wind stress curl the forcing remains zero to exclude the influence of a northern wind-driven gyre. This construction is similar to the one in Harrison and Stalos (1982).

Figures 13a–c clearly show that the premature separation at the oblique coast in Fig. 11 is an effect of the position of the wind field relative to the continent. If the gyre boundary is near the cape, premature separation occurs (Fig. 13a,b), but if the wind forcing extends far enough north (Fig. 13c), the stream begins to overshoot just as it did in Fig. 12. Incidentally, the fact that Figs. 13b and 11b do not match in every detail indicates that there is some blocking by the northern boundary in Fig. 11, but the main effect is nevertheless caused by the wind field.

Although Cox (1985) used a primitive equation model with a continental shelf, his circulation is very similar to the barotropic flat-bottom case in Fig. 13a: Böning (1989) noted that part of the western boundary current in the Cox model recirculates in a subgyre before reaching the cape and he speculated that this might be an effect of the particular form of the western wall. The results displayed in Fig. 13 support this hypothesis. The shape of the no-slip continent, the choice of $\text{curl}\tau = 0$ at the cape, and the strength of the boundary current may well have been the critical factors for the particular separation pattern found in the Cox model. Of course, among other differences between the models, Cox also used double-gyre forcing, and the influence of this will be examined in the next section.

d. Wind forcing

Locally, the contribution of the wind forcing term to the vorticity equation is very small in the western boundary current, but Fig. 13 demonstrates that the wind field can nevertheless modify the separation at a sharp corner. In this section it will be attempted to determine which aspects of the forcing affect the separation point.

As noted in section 2, the line of zero wind stress curl in the western North Atlantic roughly coincides

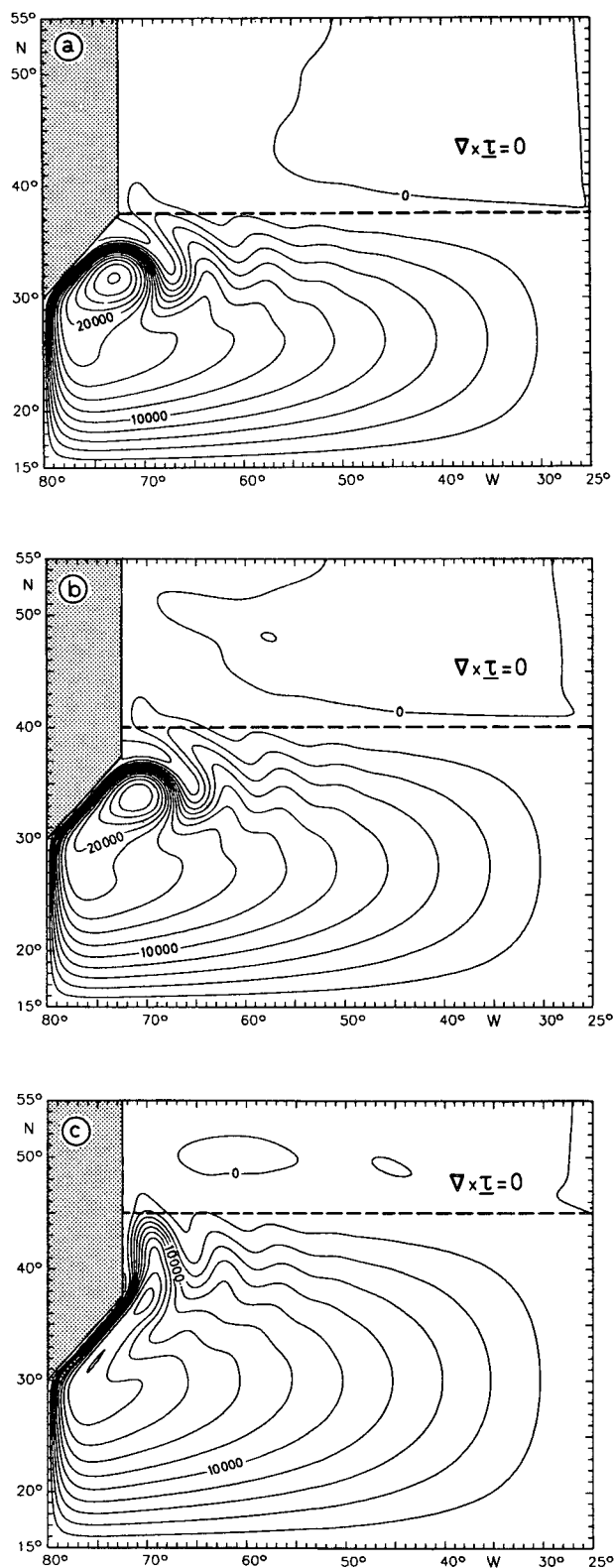


FIG. 13. Streamfunction for single-gyre forcing with $\text{curl}\tau = 0$ north of a critical latitude. Contour interval 2000 Pa; r and A_H are the same as in Fig. 3. Amplitude of wind forcing is $2\tau_0$. (a) $\text{curl}\tau = 0$ north of 37.5°N , (b) $\text{curl}\tau = 0$ north of 40.0°N , and (c) $\text{curl}\tau = 0$ north of 45.0°N .

with the course of the Gulf Stream from Cape Hatteras to Newfoundland. This naturally led to the hypothesis that the Stream's separation is a direct result of the wind forcing (Bryan 1963; Fofonoff 1981).

In Bryan's (1963) model inertial effects and an abrupt change in the orientation of the coastline were not able to produce separation. However, an asymmetrical double-gyre wind forcing with the $\text{curl}\tau = 0$ line tilted to the northeast and a straight coastline in the west gave a circulation pattern that resembled the observed Gulf Stream.

Harrison and Stalos (1982), Moro (1988), and Verron and LeProvost (1989) were able to show that for wind fields with a purely zonal orientation (in the sense that the lines of constant wind stress curl coincide with circles of latitude) the separation point at a western boundary depends mainly on the vorticity input in each of the gyres: a stronger southern gyre leads to separation north of the line of zero wind stress curl, whereas an intensified northern gyre moves the detachment point farther south. Although in these models the $\text{curl}\tau = 0$ line did not agree with the separation point, it nevertheless still determined the path of the separated current.

The model runs presented in Figs. 3, 4, and 12 show that inertial separation at a sharp corner is possible even if the line of vanishing wind stress curl is nowhere near the separation point. In fact, Fig. 13 seems to imply that the presence of $\text{curl}\tau = 0$ close to a cape can prevent inertial separation there. How are these results to be reconciled with those from straight-coast experiments? and What is the significance of the line of zero wind stress curl for the Gulf Stream's separation at Cape Hatteras?

To answer these questions, a symmetrical double-gyre forcing with $\text{curl}\tau = 0$ zonal at 35°N is chosen as an approximation to the real wind field, and a somewhat more realistic North American continent is included in the model. The result is the circulation pattern shown in Fig. 14, where the boundary current leaves the coast some distance before the cape. One might be tempted to argue that the fairly strong northern gyre forces the "Gulf Stream" to separate, but from section 4c we already know that the stream behaves the same way when there is no boundary current coming from the north. The premature separation here is a consequence of the particular choice of the southern wind gyre. Therefore, this zero-order approximation to the observed wind field does not seem very appropriate for model purposes.

Closer inspection of climatological maps of the wind stress curl (Leetma and Bunker 1978; Isemer and Hasse 1987) reveals that the $\text{curl}\tau = 0$ line off Cape Hatteras is not zonal but tilted to the northeast. So, as a first-order approximation to the observations the wind field shown in Fig. 15a was chosen. The line of zero wind stress curl still intersects the North American coast at Cape Hatteras (35°N , 75°W) but at the eastern model boundary it lies at 48°N . South of it a subtropical wind

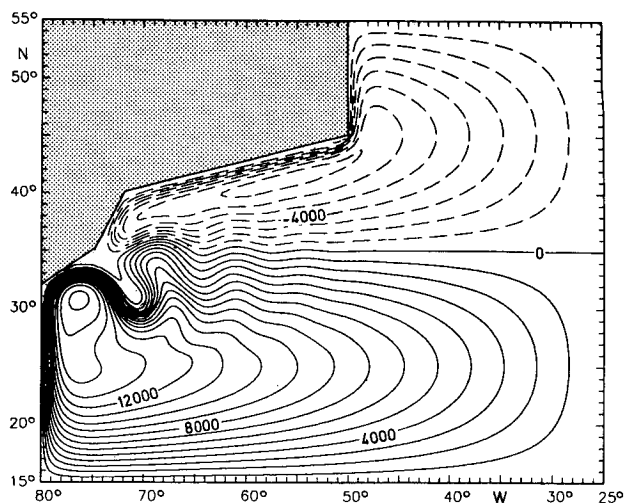


FIG. 14. Circulation for symmetric double-gyre wind forcing. Streamfunction in Pa, contour interval: 1000 Pa, wind forcing: $1.6\tau_0$, $A_H = 800 \text{ m}^2 \text{ s}^{-1}$, $r = 5 \times 10^{-7} \text{ s}^{-1}$.

gyre supplies anticyclonic vorticity to the ocean. North of the $\text{curl}\tau = 0$ line the forcing remains zero just as in Fig. 13 in order to exclude effects of a northern cyclonic gyre for the time being.

For a moderate value of wind forcing the stream now fails to separate at the cape (Fig. 15b). Instead, it forms the characteristic anticyclonic cell that is often found in ocean general circulation models, leaving the coast too far in the north and establishing a meander pattern farther downstream. If the forcing is increased by a factor of 2, the circulation looks more realistic (Fig. 15c): as in previous experiments, the stream separates and a small recirculation cell develops in the lee of "Cape Hatteras." In the instantaneous pictures (not shown here) anticyclonic rings detach from the stream and move to the north into the model's equivalent to the Middle Atlantic Bight. There they decay, leaving behind their signature even in the time-mean field (at 38°N , 70°W). According to Marshall and Marshall (1992), the rather small zonal penetration of the jet is a general feature of barotropic models.

Additional calculations revealed that in this model configuration only two possible states seem to exist: for small values of wind forcing the stream turns around the corner and the anticyclonic meander develops (Fig. 15b), whereas for strong forcing the current separates at the cape (Fig. 15c). No continuous transition between these two states was found. However, there are intermediary values of the forcing for which initially the meander state is assumed by the current, but several hundred days later the model "flips" into the separated state. Premature separation does not occur for any amplitude of the forcing although the line of vanishing wind stress curl still coincides with the cape. In Fig. 15 neither the separation point nor the course of the separated current can unequivocally be attributed to the position of $\text{curl}\tau = 0$.

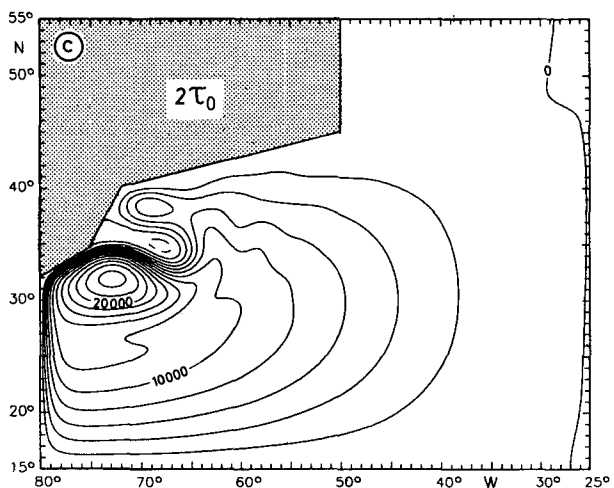
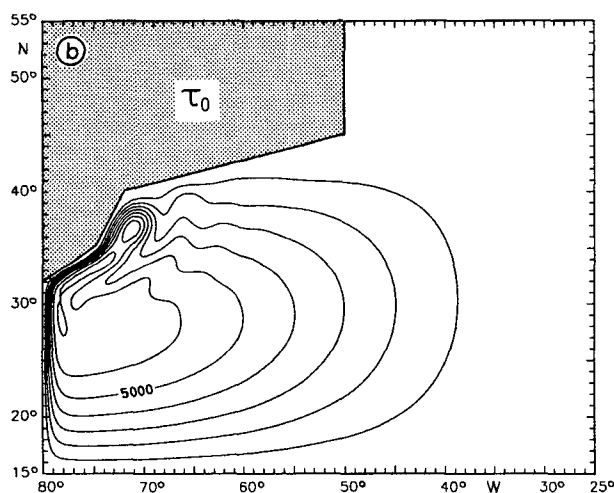
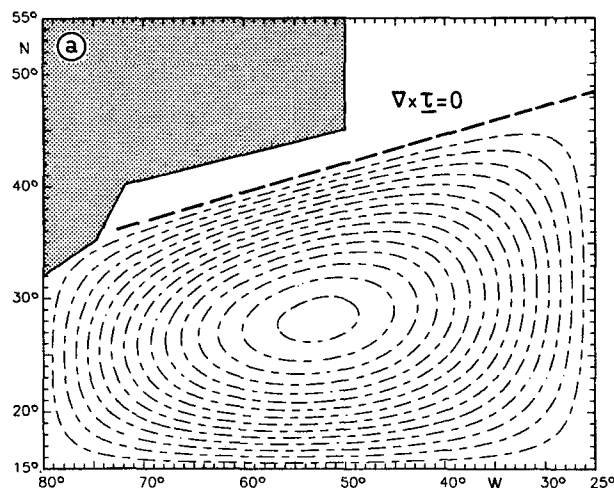


FIG. 15. Circulation for single-gyre oblique wind forcing: (a) $\text{curl}\tau$. Contour interval is $2.5 \times 10^{-10} \text{ s}^{-1}$, $\text{curl}\tau = 0$ north of the dashed line. (b) Streamfunction in Pa for τ_0 . $A_H = 1000 \text{ m}^2 \text{ s}^{-1}$, $r = 1.0 \times 10^{-7} \text{ s}^{-1}$; C.I. = 1000 Pa. (c) Streamfunction in Pa for $2\tau_0$; C.I. = 2000 Pa.

If a northern gyre is added to the model (Fig. 16), the separation behavior is not significantly altered. The linearly increasing wind forcing in the north is strong enough to produce a small gyre in the northeast corner (off "Newfoundland"), but no extension of this boundary current reaches into the "Middle Atlantic Bight." However, the "northern recirculation gyre" has slightly strengthened when compared to Fig. 15c.

The implications of these results with respect to the wind forcing are the following:

As noted already in section 4a, in the barotropic model a double-gyre forcing is not necessary to produce separation at the cape. On the other hand, if a northern wind gyre or local forcing in the Middle Atlantic Bight are included, they do not seem to alter the position of the separation point.

The time-mean separation at a cape seems to be influenced not by the local wind forcing but by its basin-

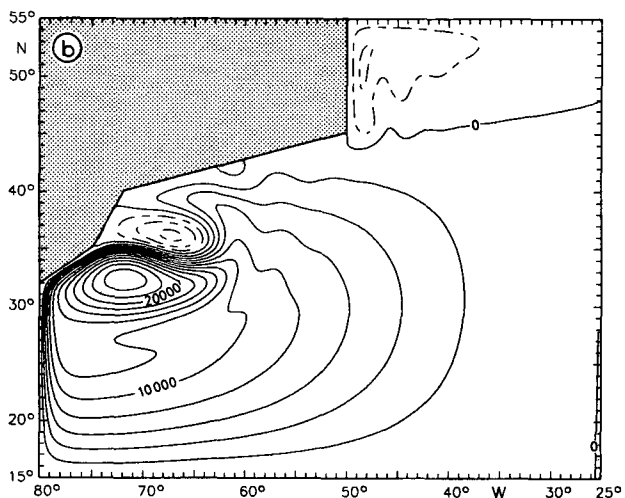
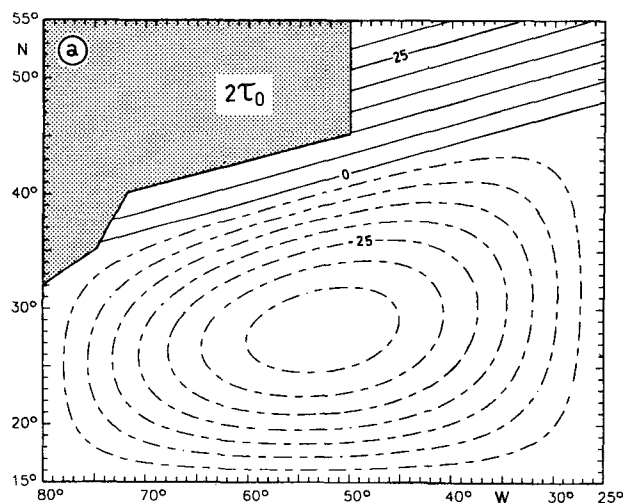


FIG. 16. Circulation for double-gyre oblique wind field: (a) $\text{curl}\tau$. Contour interval is $5.0 \times 10^{-10} \text{ s}^{-1}$. Linear increase north of $\text{curl}\tau = 0$. (b) Streamfunction in Pa for $2\tau_0$. Contour interval is 2000 Pa.

scale characteristics, and the line of zero wind stress curl ceases to have a direct influence on the separation problem. The intensity of a given horizontal wind pattern determines the magnitude of the Sverdrup transport, which in turn sets the transport of the western boundary current. Thus, different strengths of the wind gyre lead to different separation states (Fig. 15). The geometrical aspects of the subtropical wind gyre (size, position, and inclination with respect to the zonal direction) appear to control the "premature" separation, although the exact mechanism is not clear at this stage. There is some indication that the Sverdrup regime might be the controlling factor. The Sverdrup relation determines the location of the streamlines when the particles have lost the vorticity and kinetic energy gained at the western boundary. In this way it imposes a certain geographical constraint on the paths open to fluid parcels after separation from the coast. Both in Fig. 13c and in Fig. 15 the Sverdrup regime in the eastern half of the basin extends much farther north than the latitude of the cape. The constraint on fluid parcels to "meet" the streamlines there might prevent "premature" separation in these cases.

The separation behavior demonstrated in this study differs from that in straight-coast models. If the separation point in the experiments presented here were determined by the same mechanisms as at a straight coast, one would expect it to move north when the strength of the forcing is increased. However, Figs. 11 and 15 show quite the contrary effect. If the influence of the Sverdrup regime extends beyond the latitude of the cape (Fig. 15a), the coastal promontory defines a distinguished point for separation. So, different from straight-coast results, for an increase in the strength of the forcing the question is not *where* the current will separate but just *if* it will separate or not. At small Reynolds numbers the boundary current is able to follow the coastline, whereas for large Re it separates in what might be described as "inertial overshooting."

The existence of two distinct separation states means that variations of the amplitude of the large-scale wind gyre are not likely to disrupt the stream's separation at the cape, as long as the Sverdrup transport stays above some critical value. This agrees with Auer's (1987) data, which show that the separation of the Gulf Stream at Cape Hatteras is a steady feature and independent of synoptic disturbances or seasonal fluctuations of the wind forcing.

5. Conclusions

The work presented in this paper was intended as a contribution towards a better understanding of the Gulf Stream's separation at Cape Hatteras, both in numerical models and in the real ocean. A sharp convex corner was introduced into a barotropic flat-bottom model, resulting in several effects that may also be relevant to the analysis of more complex models.

One of these effects was the different separation be-

havior caused by different boundary conditions. In contrast to the no-slip condition, free slip does not allow inertial separation where fluid parcels "overshoot" the sudden change in coastline due to their large momentum. It could be shown that the failure to separate in the free-slip case lies in the nature of this boundary condition and is not a result of the particular choice of model parameters. Under the assumption that inertial separation of boundary currents should be possible at least in principle, the solutions produced with the free-slip condition (Figs. 2 and 4) are not acceptable.

The key process for separation in the no-slip case is the production of relative vorticity at the coast and its subsequent advection to the separation point, where it is then distributed to the surroundings. In the lee of the separation point, a recirculation cell is established and sustained by the separated current. The role of the nonlinear terms as a transport mechanism for vorticity explains why strong currents show clearer separation than more linear ones.

In the model, the presence of the cape together with the no-slip condition at the continent allows separation without the need for a double-gyre wind forcing. Consequently, if the real Gulf Stream also separates by "overshooting," the positive wind stress curl to the north of it is not likely to be playing a large role in this process. On the other hand, if the stream is not sufficiently nonlinear to overshoot, this cyclonic forcing may become important.

In the Munk limit examined here (width of western boundary current set by turbulent diffusion), small changes in the coefficient of bottom friction do not significantly alter the separation behavior at the cape. However, they do change the size of the recirculation cell in the lee of the continent because bottom friction is an important sink of vorticity there.

If the boundary current has to follow a zonal northern coast, "premature" separation occurs; that is, the stream leaves the boundary in an anticyclonic meander before reaching the cape. This behavior seems to be controlled by the relative magnitudes of the inertial length scale of the flow and the length scale of the coast.

At nonzonal coastlines "premature" separation can also be found, depending on the meridional position of the wind field relative to the cape. If the subtropical wind gyre extends far enough to the north, "premature" separation is replaced by overshooting.

For a more realistic wind field, that is, one that is tilted to the northeast, two distinct separation states were found in this model for different amplitudes of the wind stress curl. For weak forcing the stream follows the coastline around the cape and leaves the continent in an anticyclonic meander, whereas for strong forcing the current separates at the corner. The first path is similar to that encountered in other models; the second approximates the one taken by the real Gulf Stream. The invariance of the separation to a further increase of the wind forcing has realistic aspects because the

observed Gulf Stream's separation point does not vary with fluctuations in the wind field.

In the general case of zonally nonuniform wind forcing and irregular coastlines, separation is fairly independent of the local wind forcing near the separation point. The widespread notion that the line of zero wind stress curl determines the Gulf Stream's separation point and subsequent path cannot be supported by this simple wind-driven model.

All of the results reported in this paper were obtained without a prescribed circulation in the Middle Atlantic Bight or a density contrast between the Gulf Stream and the slope water. So, at least for the barotropic case studied in this paper, it can be concluded that the northern recirculation gyre is not an essential prerequisite for Gulf Stream separation. In fact, an inertially separating current produces a small northern recirculation gyre of its own. Although this does not agree with the conclusions of Ezer and Mellor (1992), it supports Fofonoff's (1981) theory that the circulation in the Middle Atlantic Bight may at least be partly driven by the Gulf Stream.

The conditions for separation identified in this barotropic model are not necessarily sufficient to obtain separation in other models. For example, although the WOCE-CME model (Böning et al. 1991) employs the no-slip condition, as well as realistic winds and coastlines, the Gulf Stream separation it produces is not satisfying (Bryan and Holland 1989; Treguier 1992). The behavior shown in Fig. 15 gives some indication that this lack of separation in the GFDL model might be overcome by a more nonlinear Gulf Stream, but at the moment it is not clear which of the model's free parameters has to be adjusted in order to achieve this.

Future work will have to examine if the results presented here also hold for a stratified ocean with realistic bottom topography or if different factors dominate Gulf Stream separation there.

Acknowledgments. My special thanks are due to A. Beckmann and C. Böning, who were willing to serve as a permanent "testing ground" for new ideas or theories. I am also very grateful to Prof. W. Krauss for his continuous support and trust, even at times when results did not look very promising.

This work was supported by the Deutsche Forschungsgemeinschaft, Sonderforschungsbereich 133, and Cray Research, Inc.

REFERENCES

- Auer, S. J., 1987: Five-year climatological survey of the Gulf Stream System and its associated rings. *J. Geophys. Res.*, **92**, 11 709–11 726.
- Batchelor, G. K., 1967: *An Introduction to Fluid Dynamics*. Cambridge University Press, 615 pp.
- Beardsley, R. C., and W. C. Boicourt, 1981: On estuarine and continental-shelf circulation in the Middle Atlantic Bight. *Evolution of Physical Oceanography*, B. A. Warren and C. Wunsch, Eds., The MIT Press, 623 pp.
- Bengtsson, L., and C. Temperton, 1979: Difference approximations to quasi-geostrophic models. *Numerical Methods Used in Atmospheric Models*, Vol. II, GARP Publ. Ser., 17, 340–380.
- Blandford, R. R., 1971: Boundary conditions in homogeneous ocean models. *Deep-Sea Res.*, **18**, 739–751.
- Böning, C. W., 1986: On the influence of frictional parameterization in wind-driven ocean circulation models. *Dyn. Atmos. Oceans*, **10**, 63–92.
- , 1989: Influences of a rough bottom topography on flow kinematics in an eddy-resolving circulation model. *J. Phys. Oceanogr.*, **19**, 77–97.
- , R. Döschner, and R. G. Budich, 1991: Seasonal transport variation in the western subtropical North Atlantic: Experiments with an eddy-resolving model. *J. Phys. Oceanogr.*, **21**, 1271–1289.
- Boudra, D. B., and E. P. Chassignet, 1988: Dynamics of Agulhas Retroflection and ring formation in a numerical model. Part I: The vorticity balance. *J. Phys. Oceanogr.*, **18**, 280–303.
- Bryan, F. O., and W. R. Holland, 1989: A high resolution simulation of the wind- and thermohaline-driven circulation in the North Atlantic Ocean. *Parameterization of Small-Scale Processes, Proc. 'Aha Huliko'a, Hawaiian Winter Workshop*, P. Müller and D. Henderson, Eds., Hawaii Inst. Geophys. Spec. Publ., 99–115.
- Bryan, K., 1963: A numerical investigation of a nonlinear model of a wind-driven ocean. *J. Atmos. Sci.*, **20**, 594–606.
- Cessi, P., 1990: Recirculation and separation of boundary currents. *J. Mar. Res.*, **48**, 1–35.
- , R. V. Condie, and W. R. Young, 1990: Dissipative dynamics of western boundary currents. *J. Mar. Res.*, **48**, 677–700.
- Chassignet, E. P., and P. R. Gent, 1991: The influence of boundary conditions on midlatitude jet separation in ocean numerical models. *J. Phys. Oceanogr.*, **21**, 1290–1299.
- Cherniawsky, J., and P. H. LeBlond, 1986: Rotating flows along indented coastlines. *J. Fluid Mech.*, **169**, 379–407.
- Cummins, P. F., and L. A. Mysak, 1988: A quasi-geostrophic circulation model of the Northeast Pacific. Part I: A preliminary numerical experiment. *J. Phys. Oceanogr.*, **18**, 1261–1286.
- Cox, M. D., 1985: An eddy resolving numerical model of the ventilated thermocline. *J. Phys. Oceanogr.*, **15**, 1312–1324.
- De Ruijter, W. P. M., and D. B. Boudra, 1985: The wind-driven circulation in the South Atlantic—Indian Ocean—I. Numerical experiments in a one-layer model. *Deep-Sea Res.*, **32**, 557–574.
- Ezer, T., and G. L. Mellor, 1992: A numerical study of the variability and the separation of the Gulf Stream, induced by surface atmospheric forcing and lateral boundary flows. *J. Phys. Oceanogr.*, **22**, 660–682.
- Fofonoff, N. P., 1981: The Gulf Stream System. *Evolution of Physical Oceanography*, B. A. Warren and C. Wunsch, Eds., The MIT Press, 623 pp.
- Foreman, M. G. G., and A. F. Bennett, 1988: On no-slip boundary conditions for the incompressible Navier-Stokes equations. *Dyn. Atmos. Oceans*, **12**, 47–70.
- FRAM Group, 1991: An eddy-resolving model of the Southern Ocean. *Eos, Trans. Amer. Geophys. Union*, **72**(15), 169–175.
- Haidvogel, D. B., J. C. McWilliams, and P. R. Gent, 1992: Boundary current separation in a quasigeostrophic, eddy-resolving ocean circulation model. *J. Phys. Oceanogr.*, **22**, 882–902.
- Halkin, D., and T. Rossby, 1985: The structure and transport of the Gulf Stream at 73°W. *J. Phys. Oceanogr.*, **15**, 1439–1452.
- Harrison, D. E., and S. Stalos, 1982: On the wind-driven ocean circulation. *J. Mar. Res.*, **40**, 773–791.
- Hendershott, M. C., 1987: Single layer models of the general circulation. *General Circulation of the Ocean*, H. D. I. Abarbanel and W. R. Young, Eds., Springer-Verlag, 291 pp.
- Hogg, N. G., R. S. Pickart, R. M. Hendry, and W. J. Smethie, Jr., 1986: The northern recirculation gyre of the Gulf Stream. *Deep-Sea Res.*, **33**, 1139–1165.
- Holland, W. R., 1973: Baroclinic and topographic influences on the transport in western boundary currents. *Geophys. Fluid Dyn.*, **4**, 187–210.
- , 1986: Quasigeostrophic modelling of eddy-resolved ocean circulation. *Advanced Physical Oceanographic Numerical Modelling*, J. J. O'Brien, Ed., Reidel, 608 pp.

- , 1987: A limited area model for the Gulf Stream region. *Three-Dimensional Models of Marine and Estuarine Dynamics*, J. C. J. Nihoul and B. M. Jamart, Eds., Elsevier, 629 pp.
- , and L. B. Lin, 1975: On the generation of mesoscale eddies and their contribution to the oceanic general circulation. II: A parameter study. *J. Phys. Oceanogr.*, **5**, 658–669.
- Isemer, H.-J., and L. Hasse, 1987: *The Bunker Climate Atlas of the North Atlantic Ocean*. Vol. 2. *Air-Sea Interactions*. Springer-Verlag, 252 pp.
- Leaman, K. D., E. Johns, and T. Rossby, 1989: The average distribution of volume transport and potential vorticity with temperature at three sections across the Gulf Stream. *J. Phys. Oceanogr.*, **19**, 36–51.
- Leetmaa, A., and A. F. Bunker, 1978: Updated charts of the mean annual wind stress, convergences in the Ekman Layers and Sverdrup transports in the North Atlantic. *J. Mar. Res.*, **36**, 311–322.
- Luyten, J. R., and A. R. Robinson, 1974: Transient Gulf Stream meandering. Part II: Analysis via a quasi-geostrophic time-dependent model. *J. Phys. Oceanogr.*, **4**, 256–269.
- MacVeigh, J. P., B. Barnier, and C. LeProvost, 1987: Spectral and empirical orthogonal function analysis of four years of European Centre for Medium Range Weather Forecasts wind stress curl over the North Atlantic Ocean. *J. Geophys. Res.*, **92**, 13 141–13 152.
- Marshall, D., and J. Marshall, 1992: Zonal penetration scale of mid-latitude oceanic jets. *J. Phys. Oceanogr.*, **22**, 1018–1032.
- Marshall, J. C., 1984: Eddy-mean-flow interaction in a barotropic ocean model. *Quart. J. Roy. Meteor. Soc.*, **110**, 573–590.
- Maul, G. A., P. W. DeWitt, A. Yanaway, and S. R. Baig, 1978: Geostationary satellite observations of Gulf Stream meanders: Infrared measurements and time series analysis. *J. Geophys. Res.*, **20**, 6123–6135.
- Mellor, G. L., and T. Ezer, 1991: A Gulf Stream model and an altimetry assimilation scheme. *J. Geophys. Res.*, **96**, 8779–8795.
- Moro, B., 1988: On the nonlinear Munk model. I: Steady flows. *Dyn. Atmos. Oceans*, **12**, 259–287.
- Pedlosky, J., 1979: *Geophysical Fluid Dynamics*. Springer-Verlag, 624 pp.
- Rhines, P. B., and R. Schopp, 1991: The wind-driven circulation: Quasi-geostrophic simulations and theory for nonsymmetric winds. *J. Phys. Oceanogr.*, **21**, 1438–1469.
- Richardson, P. L., 1977: On the crossover between the Gulf Stream and the Western Boundary Undercurrent. *Deep-Sea Res.*, **24**, 139–159.
- , 1985: Average velocity and transport of the Gulf Stream near 55°W. *J. Mar. Res.*, **43**, 83–111.
- , and J. A. Knauss, 1971: Gulf Stream and Western Boundary Undercurrent observations at Cape Hatteras. *Deep-Sea Res.*, **18**, 1089–1109.
- Roache, P. J., 1976: *Computational Fluid Dynamics*. Hermosa, 446 pp.
- Robinson, A. R., and P. P. Niiler, 1967: The theory of free inertial currents. I: Path and structure. *Tellus*, **19**, 269–291.
- Thompson, J. D., and W. J. Schmitz, Jr., 1989: A limited-area model of the Gulf-Stream: Design, initial experiments, and model-data intercomparison. *J. Phys. Oceanogr.*, **19**, 791–814.
- Treguier, A. M., 1992: Kinetic energy analysis of an eddy resolving, primitive equation model of the North Atlantic. *J. Geophys. Res.*, **97**, 687–701.
- Veronis, G., 1966: Wind-driven ocean circulation—Part 2. Numerical solutions of the non-linear problem. *Deep-Sea Res.*, **13**, 31–55.
- Verron, J., and C. LeProvost, 1989: Asymmetrical wind forcing driving some numerical eddy-resolving general circulation experiments. *Mesoscale/Synoptic Coherent Structures in Geophysical Turbulence*, J. C. J. Nihoul and B. M. Jamart, Eds., Elsevier, 841 pp.
- Warren, B. A., 1963: Topographic influences on the path of the Gulf Stream. *Tellus*, **15**, 168–183.
- Werner, F. E., A. Cantos-Figueroa, and G. Parrilla, 1988: A sensitivity study of reduced-gravity channel flows with application to the Alboran Sea. *J. Phys. Oceanogr.*, **18**, 373–383.